18th IFHTSE CONGRESS
International Federation for Heat Treatment and Surface Engineering
IFHTSE

ANAIS
PROCEEDINGS
ISSN 1516-392X

# SURFACE TREATMENT OF LOW-COST BETA TITANIUM ALLOY TO COMBAT WEAR[1]

E. Redmore[2]
X. Li[3]
H. Dong[3]

## Abstract

The development of an effective ceramic conversion treatment of TIMETAL LCB (Ti-6.8Mo-4.5Fe-1.5Al) has been investigated. Various characterisation methods were used to analyse samples in order to identify the best process conditions including SEM, EDX, XRD, GDS, micro-indentation and scratch testing. The results show that the tribological properties of the TIMETAL LCB alloy have been significantly enhanced by the new ceramic conversion treatment specifically developed for beta alloys. The improved friction and wear properties can be attributed to the low-friction $TiO_2$ surface layer supported by an oxygen diffusion hardened case up to a depth of ~70µm.

**Keywords**: TIMETAL LCB; Ceramic conversion; Wear; Friction.

## EMERJA TRATAMENTO DE LIGA DE BAIXO CUSTO DE TITÂNIO DE BETA COMBATER USO

## Resumo

O desenvolvimento de um tratamento de conversão cerâmico eficaz de TIMETAL LCB (Ti-6.8Mo-4.5Fe-1.5Al) foi investigado. Vários métodos de caracterização foram usados para analisar amostras para identificar as melhores condições de processo inclusive SEM, EDX, XRD, GDS, micro-recuo e arranhão testando. Os resultados mostram que as propriedades de tribological da liga de LCB DE TIMETAL significativamente foram melhoradas pelo novo tratamento cerâmico de conversão especificamente desenvolvido para ligas de beta. A fricção melhorada e propriedades de uso podem ser atribuídas à camada de superfície TiO2 de baixo-fricção apoiada por uma difusão de oxigênio endureceu caso até uma profundidade de ~70µm.

**Palavras-chave**: TIMETAL LCB; Conversão cerâmica; Fricção

---

*[1] Technical contribution to the 18th IFHTSE Congress - International Federation for Heat Treatment and Surface Engineering, 2010 July 26-30th, Rio de Janeiro, RJ, Brazil.*

*[2] Corresponding author. Tel.: +44-7840151275; email: ellyredmore622@hotmail.com. Degree: Masters in Materials Engineering.*

*[3] School of Metallurgy and Materials, University of Birmingham, UK. PhD.*

## 1 INTRODUCTION

The non-aerospace use of titanium alloys (such as in the motor sports industry) has become increasingly popular over last 20 years or so due to their light weight, high ductility and high strength in conjunction with excellent corrosion resistance and outstanding biocompatibility. Titanium alloys are normally classified by its structure into the groups of alpha, alpha-beta and beta alloys. Advantages of β phase alloys include excellent workability, good hardenability, high corrosion resistance and excellent fatigue/ crack propagation behaviour.(1) TIMETAL LCB (Ti-6.8Mo-4.5Fe-1.5Al) is a low-cost beta (LCB) alloy developed specifically for non-aerospace (e.g. automotive) applications. TIMETAL LCB has been found to have a better combination of high strength (UTS>1500 MPa) and good ductility (total elongation >8%) than many other β alloys.(1)

However, it has been reported that the natural oxide film that forms on titanium and its alloys has been found to easily rub off, thus leaving their substrate in a state of high friction and low wear resistance.(2) Consequently, titanium and its alloys are characterised by inferior tribological properties including a high and unstable coefficient of friction and a strong scuffing tendency.(3) This is a problem for titanium and its alloys in all tribological applications, and surface engineering is an essential requirement for the tribological applications of titanium components.

To this end, many surface engineering methods have been researched to combat the poor tribological properties of titanium and its alloys. These range from surface coatings such as PVD and plasma electrolytic oxidation to surface modifications such as ion implantation, plasma nitriding and thermal oxidation.(4) However, there is little research on the surface engineering of TIMETAL LCB alloy within the current literature which is an issue needing to be addressed.

Research carried out by Dong and Bell(2) on the titanium alloy Ti6-Al4-V demonstrated the effectiveness of the thermal oxidation (TO) treatment in enhancing the wear resistance of the alpha/beta alloy. During the treatment, the titanium alloy surface was converted through controlled thermal oxidation processes into a diffusionally bonded ceramic (rutile $TiO_2$) layer and an oxygen strengthened diffusion zone underneath. Typical TO-treatment for most α+β alloys is normally carried out at about 600°C in air for a long time (50-100h).

However, this process cannot be directly applied to the TIMET LCB alloy since it is a metastable beta alloy. The long-time TO treatment at high-temperature will cause undue growth of the beta grains and excessive precipitation of the alpha phase, thus leading to the degradation of the core mechanical properties of the β-alloy.

Therefore, the aim of this research was to enhance the tribological properties of TIMETAL LCB alloy without evoking a loss of core mechanical properties through developing new surface engineering processes based on integration of bulk heat treatment with surface ceramic conversion.

## 2 EXPERIMENTAL

The TIMET LCB titanium alloy supplied by Titanium Metals Corporation for research purposes was used as the substrate material, which was solution treated and aged for 4 hours at 565.5°C. The nominal composition of the material was (wt %): 6.8%Mo, 4.5%Fe, 1.5% Al and balance Ti.

A rod of 25mm in diameter was cut into 5mm sections to produce the coupon samples. Standard sample preparation procedure was used to grind the surface of the samples up to 1200 grit, cleaned with acetone and dried under hot air.

Samples were loaded into an Elite electric furnace, heated at a ramp rate of 10°C/min from 23 °C to 850 °C and then held for either 0.5 or 6 hours. Immediately after holding time finished, samples were removed from the furnace and dropped into cold water for quenching. Because of the undue damage of the 6h solution treated surfaces, 0.5 hours was chosen as the best length of time for the solution treatment. Then, solution treated samples were aged at 500, 550 or 600 °C for 4, 8, 16 or 32 hours. A summary of the treatment matrix and sample code is given in Table 1.

Metallographic cross-sections of the treated samples were prepared by cutting, mounting, grinding up to 1200 grit, polishing using 6 µm and 1 µm diamond paste and finished with ½ µm polishing using colloidal silica. For microscopic observation, some stubs were etched in a solution of 2% HF, 10% HNO3, and 88% $H_2O$.

**Table 1.** Treatment parameters and specimen codes

| Specimen | Solution treatment time (at 850°C), hrs | Aging temperature ,°C | Aging time, hrs |
|---|---|---|---|
| ST6 | 6 | - | - |
| ST0.5 | 0.5 | - | - |
| STA500_8 | 0.5 | 500 | 8 |
| STA550_8 | 0.5 | 550 | 8 |
| STA600_8 | 0.5 | 600 | 8 |
| STA500_4 | 0.5 | 500 | 4 |
| STA500_8 | 0.5 | 500 | 8 |
| STA500_16 | 0.5 | 500 | 16 |
| STA500_32 | 0.5 | 500 | 32 |

Surfaces and cross-sections of the samples were examined under a Phillips XL30 scanning electron microscope (SEM) equipped with energy dispersive X-ray spectroscopy (EDX) for composition analysis. The phase constituents of the as-received and treated samples were studied by X-ray diffraction (XRD) from 20-100°. A Spectrumat GDS-750 was used for glow discharge spectroscopy (GDS) to enable the concentration percentage of elements in the first few microns of the sample surface to be collected.

Polished cross-sections of the samples were used to generate hardness-depth profiles from the oxygen diffusion zone beneath the top oxide layer. A load of 100g was applied via a Vickers indenter. Scratch tests were conducted to assess the bonding of the oxide layer to the hardened substrate. A Rockwell diamond indenter with a 200µm radius tip was drawn across the surface at a linear velocity of 10 mm/min and loading rate of 100 N/min from 0.5 to 40 N.

Reciprocating pin-on-disc sliding wear tests were conducted using the TE79 multi-axis tribology machine with an 8mm tungsten carbide ball as the counterpart under a load of 10N with an amplitude of 10mm and an average sliding speed of 10 mm.$s^{-1}$. The resultant wear tracks were measured using a profilometer and the wear loss was calculated by integrating the cross-sectional area of the wear track and then timing the length of wear track. The coefficient of friction was calculated according to the recorded friction force and the applied normal load. Post-examination of the wear tracks was carried out to investigate the wear mechanism involved.

## 3 RESULTS AND DISCUSSION

### 3.1 Effect of Solution Treatment Time

SEM and XRD analysis had confirmed that as-received TIMETAL LCB was dominated by beta phase with small amount of alpha in the beta matrix. Alpha-phase precipitates were most evident at the grain boundaries in SEM micrographs (Fig. 1) as the black areas. This was confirmed by EDX when lower molybdenum content was observed in these areas; being a beta stabiliser, Mo was lean in the alpha phases. The hardness of the as-received TIMETAL LCB material was measured to be about 500HV0.1.

SEM observations of the cross section (Fig.2) of the treated samples revealed a top white layer followed by a case with two phases (Fig.2b). It was also found that the grains and grain boundaries in the substrate of the solution treated sample (see the lower part of Fig. 2a) were no longer outlined in black precipitates as observed in Fig.1 for the as received material. This is in line with the finding that the intensity of the alpha phase peaks from the solution treated sample reduced as compared with that for the as-received material (Fig.3). Clearly, the alpha precipitates were transformed into beta during the solution treatment.

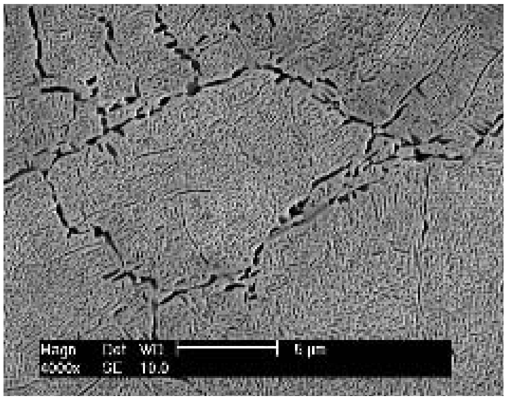

**Figure 1.** SEM microstructure of as-received TIMETAL LCB material.

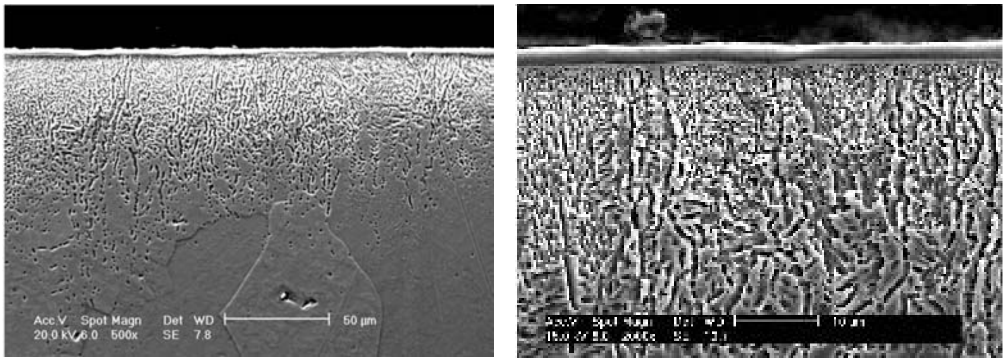

**Figure 2.** SEM images of the surface layers at low (a) and high (b) magnification of sample ST0.5.

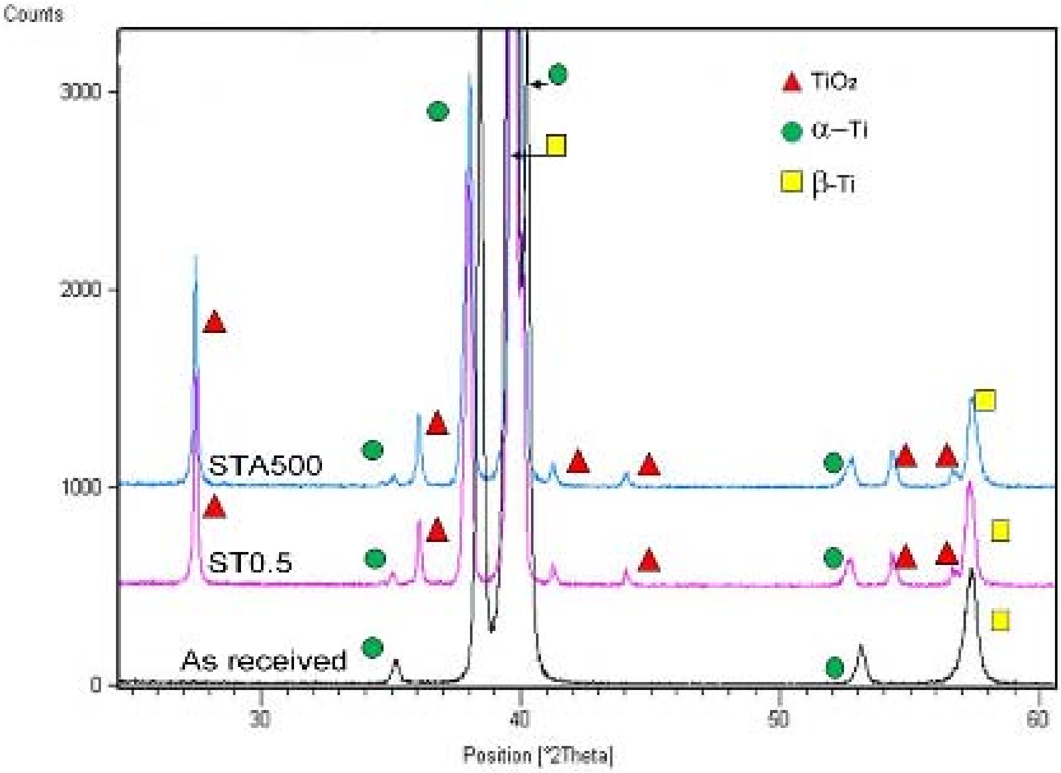

**Figure 3.** XRD patterns from three TIMETAL LCB samples; as- received (untreated) ST0.5 and STA500.

Indexing of the peaks shown in the XRD charts (Fig. 3) also show that $TiO_2$ rutile oxide was formed because of oxidation during the solution treatment. The two-phase microstructure formed beneath the surface oxide layer could be attributed to the formation an oxygen diffusion zone (ODZ) due to inward diffusion of oxygen (Fig. 4). This is because oxygen is known to be a strong alpha stabiliser for titanium. This is also supported the alpha peaks observed for the solution treated sample.

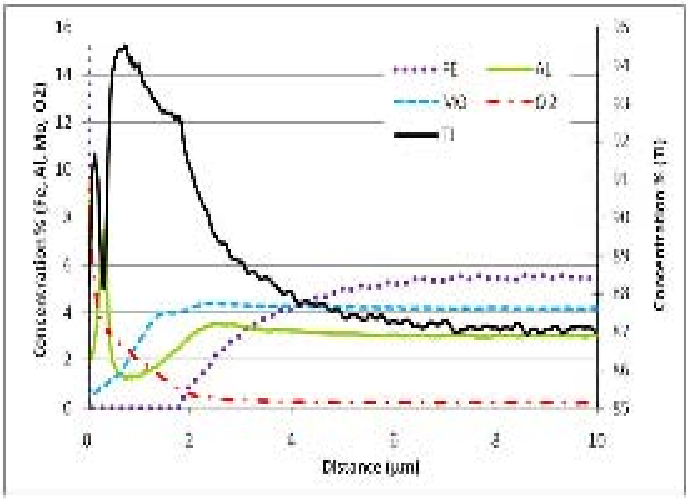

**Figure 4.** GDS depth profile of ST0.5 sample, showing elements distribution along depth.

It is of interest to find that although ST0.5 was found to have a far smaller oxygen diffusion zone than ST6, the former has a slightly thicker oxide layer than the later (Fig.5). This is mainly because oxygen diffusion distance and thus the thickness of the ODZ, depends on the treatment time and a longer treatment would produce a thicker ODZ case. However, a long-time treatment may have caused spallation of the superficial oxide layer (similar to that shown in Fig. 6), thus giving rise to a thinner final oxide layer.

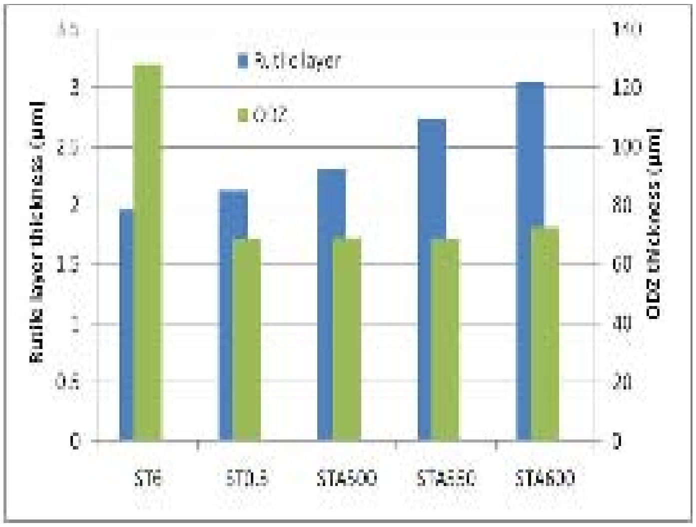

**Figure 5.** Thicknesses of the rutile $TiO_2$ layer and average oxygen diffusion zone (ODZ) from all treated samples thus far.

As has been shown in Fig.3, XRD of the as-received material showed both cubic structure titanium beta peaks and hexagonal structure titanium alpha peaks. The significant shift to the right of the beta titanium peaks from standardised values was an effect caused by the smaller atoms of the substitutional element of Mo within the Ti alloy reducing the lattice structure size. On the other hand, the alpha peaks were shafted to the left because of interstitial solid solution of oxygen, which is a strong alpha stabiliser.

The GDS depth profile (Fig. 4) of ST0.5 reveals a strong presence of aluminium just under the $TiO_2$ layer in the first micron of the sample surface. It is known that $TiO_2$ can only contain a very small amount of Al so this is likely that Al was pushed out of the rutile layer; either back into the substrate or onto the surface. This is confirmed by aluminium only peaking when titanium drops. It appears that the surface structure could be made up of a very thin layer of titanium dioxide ($TiO_2$) followed by a very thin layer of alumina ($Al_2O_3$) on the top of a relatively thick layer of $TiO_2$. This is in agreement with Rastkar and Bell(5) who found that an alumina rich intermediate layer formed near the topmost surface layer. More detailed TEM work is being undertaking to further clarify this.

Based on the above results, it was decided that 0.5h was chosen as the solution treatment time for the rest of the research because it can produce a rutile oxide layer with a good surface finish, a strong bonding to the substrate and relatively high toughness.

### 3.2 Effect of Aging Temperature

The ST0.5 samples were aged at 500, 550 or 600 °C for 8 hours. On visual observation of the samples, the two higher temperature treatments had caused the oxide layer to become very brittle and flaked off upon handling (Fig. 6). SEM observation revealed firstly that the bonding between the oxide layer and the substrate was weak on STA550 and STA600, as indicated by the black space between the oxide and substrate (Fig. 7). Secondly, alpha phase precipitates had once again formed at the grain boundaries in the substrate. Fig. 7a shows a grain below the oxygen diffusion zone outlined in black. At higher magnification and by EDX analysis these were confirmed as alpha phase precipitates.

From solution treatment for 0.5 hrs through to aging at the three different temperatures, very little change occurred in the oxygen diffusion zone thickness (Fig. 5). A steady increase in rutile layer thickness occurred, going from 2.15 μm after solution treatment to 3.05 μm after aging for 8 hours at 600°C.

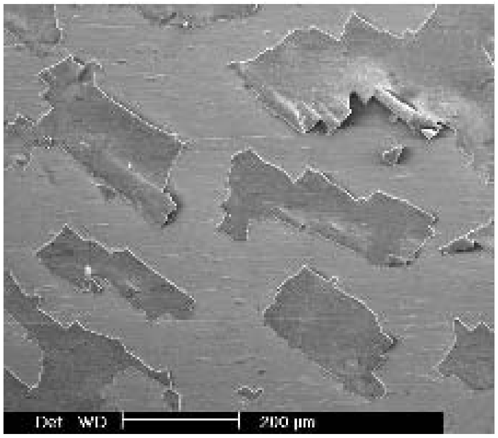

**Figure 6.** SEM image of STA550 surface.

Comparison of XRD patterns of samples STA500, STA550 and STA600 showed that they were formed of similar phases and typical pattern of STA 500 has been included in Fig. 3. The differences observed between different aging temperatures were the position of the beta peaks, which shifted to the lower angles when aging temperature is higher. As the titanium is heated at an increasing temperature, more $TiO_2$ forms on the surface of the sample which leaves an increased weight percentage of molybdenum within the titanium matrix. This lowers the d-spacing of the beta phase because of the small atomic size of Mo.

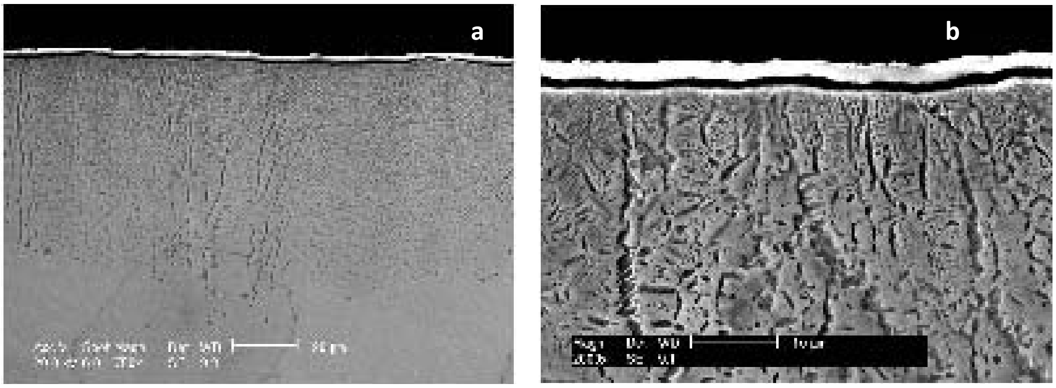

**Figure 7.** SEM micrographs of STA550 at low (a) and high (b) magnification.

The microhardness of the aged samples showed that STA600 had a higher initial hardness, but this then fell quickly with the depth, as did that of STA550, whilst the hardness of STA500 reduced gradually within the oxygen diffusion zone (Fig. 8). Nearly all the visible error bars are from STA600 indicating non-homogeneous mechanical properties. This is caused by over-aging and the newly formed precipitates being too different from the parent material.

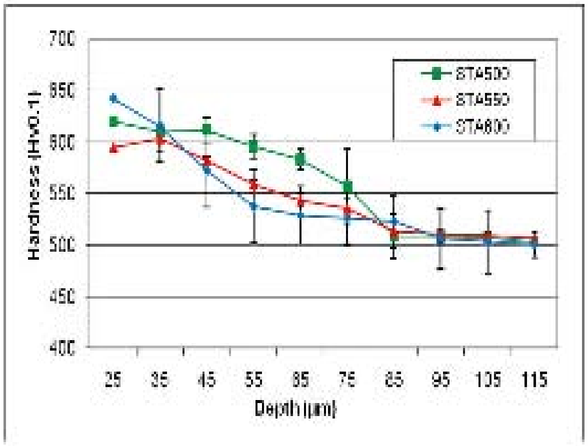

**Figure 8.** Temperature effect on surface layer hardness.

Mechanical testing examined how the samples acted under static and dynamic loadings. Static loading was carried out in the form of load bearing capacity tests, using increasing loads on the microindenter. The hardness at each load was recorded and the indents were imaged (Fig. 9). The oxide layer on STA500 did not crack until a load of 300g was applied, whereas STA550 and STA600 both cracked at 100g loads. The indent in STA500 (Fig.9a) caused circular cracking or 'nesting' cracking. This occurs when the substrate underneath is not hard enough to support the load on the oxide layer but the bonding between the oxide layer and the substrate is good.  On the other hand, partial spallation (Fig.9b) and severe spallation (Fig. 9c) occurred to ST550 and ST600 respectively, clear indication of poor bonding strength. Consequently, 500 °C was chosen as the optimal aging temperature for this study.

**Figure 9.** Cracking caused by Vickers indenter at 500g load on surface of STA500 (a), STA550 (b) and STA600 (c).

### 3.3 Effect of Aging Time

In order to investigate the effect of aging time, ST0.5 samples were aged at 500°C for 4, 8, 16 or 32 hours. All aged samples had a good surface finish and only small differences were seen in the thicknesses of rutile layers (Fig. 10). The thickness of the ODZ increased slowly but surely, with the aging time. However, compared with aging temperature, aging time possessed a much weaker effect on the thickness of the ODZ (Fig. 5 vs. Fig. 10).

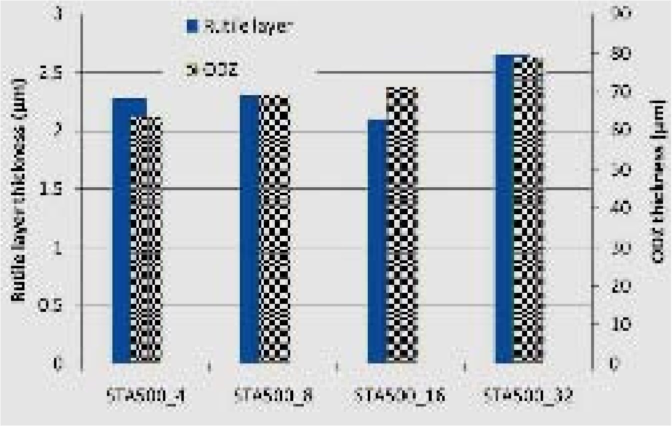

**Figure 10.** $TiO_2$ layer and oxygen diffusion zone (ODZ) thickness of differing time aged samples STA500.

Fig. 11 shows the effect of aging time on the hardness of the substrate. It can be seen that the hardness of the substrate of STA500_4 and STA500_8 is very close to that of the as-received material; however, softening was observed from the substrate of STA500_16 and STA500_32. This implies that these two samples were probably 'over-aged'.(8)

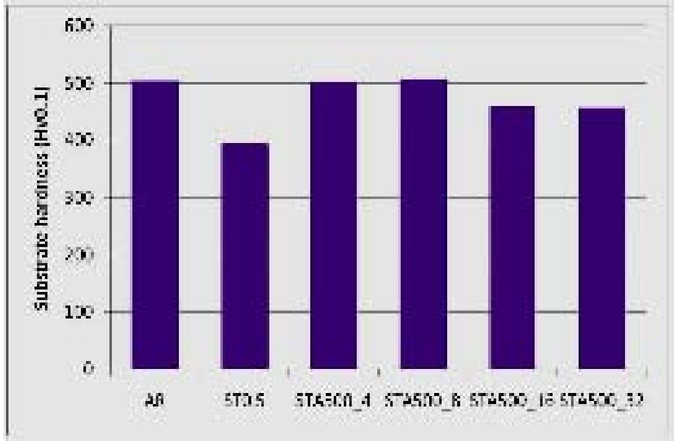

**Figure 11.** Substrate hardness of the samples with different treatment conditions.

Load bearing capacity tests revealed that with a longer aging time, the oxide film increased in brittleness. For example, STA500_4 had a high critical load of 500g, whilst STA500_32 cracked at just 100g. This is also supported by the results of scratch tests. Judging by the first derivative of the friction force curves recorded, the critical load is about 22, 14 and 10N for STA500_4, 8 and 16 respectively (Fig. 12). Below the critical load, all the friction force curves are relatively smooth; above the critical load, the friction force curves not only became fluctuating but their slope became steeper. This is largely because the surface rutile oxide layer has low friction and therefore the friction would significantly increase once the oxide layer was removed.

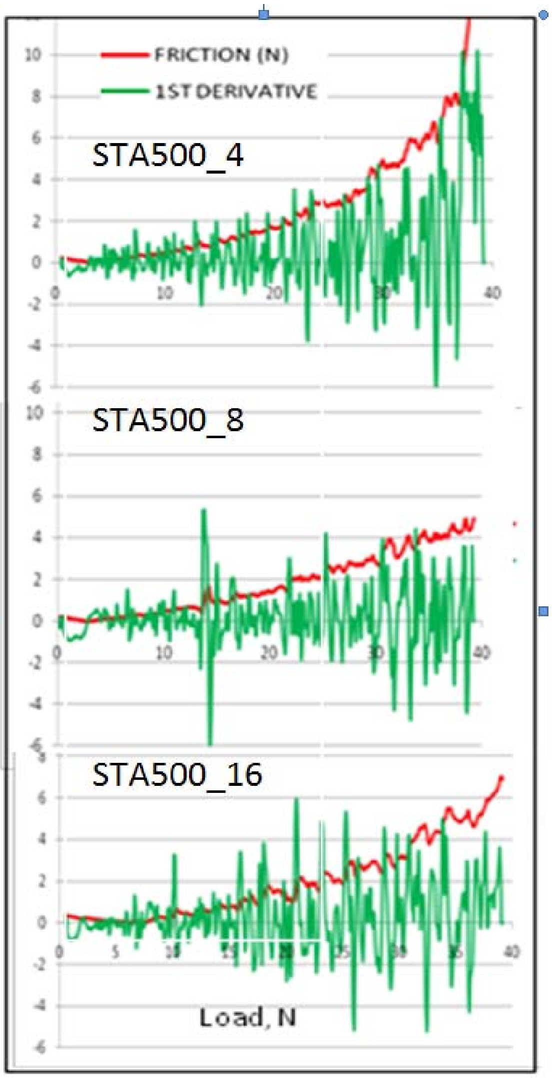

**Figure 12.** Scratch profiles of samples STA500_4, 8 and 16.

SEM observations revealed that spallation occurred once the applied load was beyond the critical load. It is know from the Fig. 10 that the thickness and thus the mechanical support of the ODZ increased with the aging time, and therefore, the failure of the surface oxide is likely related to the reduced bonding between the top oxide layer and the ODZ.(7)

### 3.4 Tribological Properties

Fig.13 shows the profiles of typical wear tracks formed during the pin-on-disc reciprocating sliding wear tests. The as-received sample experienced severe wear loss as evidenced by the wide (1.8mm) and deep (~14 microns) of the wear track; in contrast, the wear track formed on the treated surfaces was very narrow and shallow. Quantitative wear test results are summarised in Fig. 14.

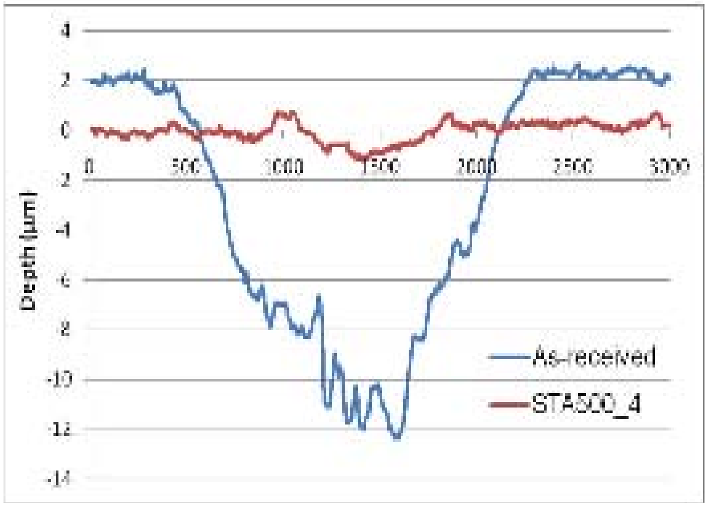

**Figure 13.** Wear track profiles of as-received and STA500_4 samples, using a 10N load for 500 cycles.

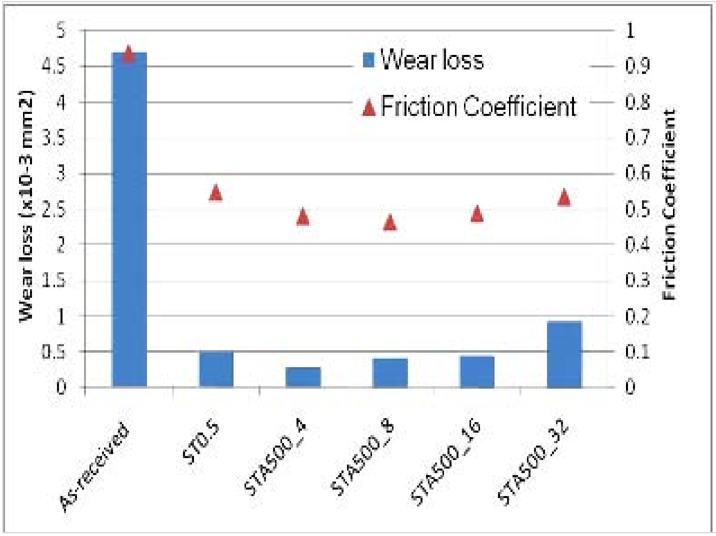

**Figure 14.** Wear loss and friction coefficient of wear tested samples, 10N load for 500 cycles.

Clearly, compared with the as-received material, ST0.5, STA500_4, 8, 16 and 32 samples all showed significantly reduced wear. Among these treated samples, STA500_4 possessed the best wear resistance and STA500_32 turned to be the worst.

As shown in Fig. 14, the friction coefficient of the as-received TIMETAL LCB is above 0.9 whilst all surface treated samples showed a significantly reduced friction coefficient of about 0.5. This is because rutile $TiO_2$ has been reported to have low critical shear strength.(8)

SEM observations of wear scars showed that severe wear occurred to the as-received material as evidenced by the large adhesive craters and parallel scratches within the wear track formed in the sample surface (Fig. 15a). As with all other titanium alloys TIMETAL LCB has a very low d-bond character.(2) Therefore, TIMETAL LCB is very active and tends to form strong adhesion on cold weld of junctions. In addition, as a beta alloy, TIMETAL LCB has good ductility and toughness and hence strong growth of the junctions is expected. As a result, TIMETAL LCB showed very strong adhesive wear tendency. TIMETAL LCB was transferred to the counterface and work hardened during the subsequent contact, which caused abrasive wear of the TIMETAL LCB surfaces.

The morphology of the wear track formed in the surface treated samples is extremely different. Fig. 15b depicts the wear track morphology for tested STA500_8, and no signs of adhesive wear or abrasive wear could be observed. This is mainly because the surface STA500_8 has been converted from metallic Ti into ceramic rutile layer.

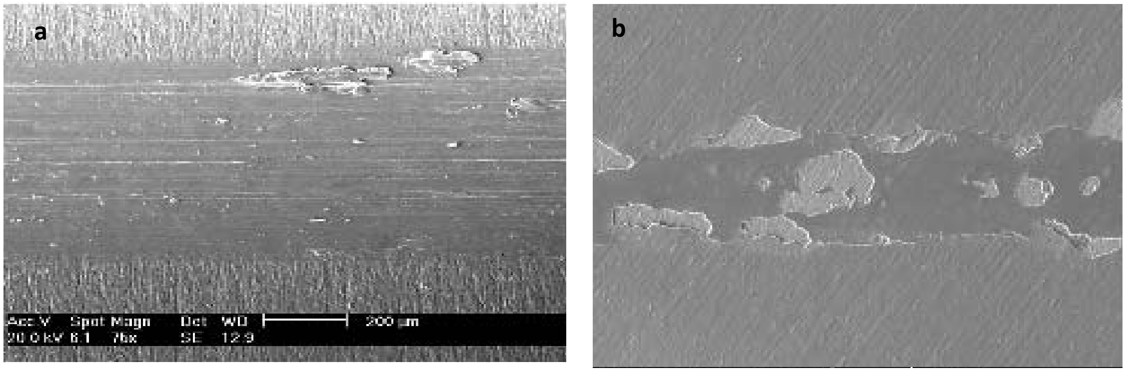

**Figure 15.** Wear scars of as-received material (a) and STA500_8 (b).

This not only can increase the surface hardness and hence reduce abrasive wear but also can improve the tribological compatibility and thus reduce adhesive wear. Localised spallation can be found from the wear track formed in STA500_8. Although the mechanism behind is still under investigation, this is most probably related to interface failure under repeated stressing and fatigue wear(2) under the current wear conditions.

## 4 SUMMARY AND CONCLUSIONS

Results show that the new ceramic conversion treatment developed from the research based on integration of bulk and surface treatment is a suitable method of surface engineering for the improvement of wear and friction resistance in TIMETAL LCB (Ti-6.8Mo-4.6Fe-1.5Al) without evoking a loss of core mechanical properties. Based on systematic processing and characterisation, it has been found that the optimal treatment parameters are solution treatment at 850°C for 0.5 hours followed by aging at 500 °C for 4-8 hours. Improvement in wear and friction properties of TIMETAL LCB can be attributed to the formation of a low-friction rutile oxide layer supported by an oxygen diffusion hardened case.

## Acknowledgements

The authors would like to thank Titanium Metals Corporation for donating the LCB titanium at no cost. One author would like to thank the University of Birmingham, England for tuition fees funding and the Engineering and Physical Sciences Research Council for the research studentship.

## REFERENCES

1 Ivansishin, OM, Markovsky, PE, Matviychuk, YuV, Semiatin, SL, Ward, CH, Fox, S. 2007 'A comparative study of the mechanical properties of high-strength β-titanium alloys' Journal of Alloys and Compounds, vol. 457, pp. 296-309

2 Dong, H, Bell, T. 2000 'Enhanced wear resistance of titanium surfaces by a new thermal oxidation treatment' Wear, vol. 238, pp. 131-137

3 Dong, H, Bell, T, Mynott, A. 1999 'Surface engineering of titanium alloys for the motorsports industry' Sports Engineering, vol. 2, pp. 213- 219

4 Dong, H. Surface Engineering of Light Alloys – Aluminium, Magnesium and Titanium Alloys, Woodhead Publishing Ltd, Cambridge, UK, May 2010 (ISBN 978-1-84569-537-8)

5 Rastkar, AR, Bell, T. 2005 'Characterisation and tribological performance of oxide layers on a gamma based titanium aluminide' Wear, vol. 258, pp.1616-1624

6 Sritharan, T, Chandel, RS. 1997 'Phenomena in interrupted tensile tests of heat treated aluminium alloy 6061' *Acta Materials*, vol. 45, pp. 3155-3161

7 Bull, SJ. 1997 'Failure mode maps in the thin film scratch adhesion test ' *Tribology International*, vol. 30, no.7, pp. 491-498

8 Diebold, U. 2003 'The surface science of titanium dioxide' Surface Science Reports, vol. 48, issues 5-8, pp. 53-229